Journal of Alloys and Compounds 509S (2011) S328–S333

Contents lists available at ScienceDirect

Journal of Alloys and Compounds

journal homepage: www.elsevier.com/locate/jallcom

First principles investigation of the substitutional doping of Mn in Mg_2Ni phase and the electronic structure of Mg_3MnNi_2 phase

L.W. Huang*, O. Elkedim*, R. Hamzaoui

FEMTO-ST, MN2S, Université de Technologie de Belfort-Montbéliard, Site de Sévenans, 90010 Belfort cedex, France

A R T I C L E I N F O

Article history:
Received 4 July 2010
Received in revised form 5 August 2010
Accepted 25 August 2010
Available online 28 September 2010

Keywords:
First principles calculation
Mn-doped Mg_2Ni
Mg_3MnNi_2
Enthalpy of formation
Electronic structure

A B S T R A C T

The substitutional doping of Mn in Mg_2Ni phase and the electronic structure of Mg_3MnNi_2 phase have been investigated by first principles density functional theory calculations. The calculation of enthalpy of formation shows that among the four different lattice sites of Mg(6f), Mg(6i), Ni(3b) and Ni(3d) in Mg_2Ni unit cell, the most preferable site of substitution of Mn in Mg_2Ni lattice has been confirmed to be Mg(6i) lattice site. The constructed $Mg_9Mn_{3Mg(6i)}Ni_6$ structure by replacing 3 Mg atoms at Mg(6i) lattice sites with 3 Mn atoms in the Mg_2Ni unit cell is less stable. In contrast, the cubic Mg_3MnNi_2 phase that has the same composition as that of $Mg_9Mn_{3Mg(6i)}Ni_6$ structure possesses good stability. Analysis of density of states (DOS) indicates that there is a strong hybridization between Mg s, Mg p and Ni d electrons, which is dominant in controlling the structural stability of pure and Mn-doped Mg_2Ni phases. The Mn-substitution in Mg_2Ni unit cell weakens the interaction between Mg s, Mg p and Ni d electrons, especially for $Mg_9Mn_{3Mg(6i)}Ni_6$ phase. The cubic Mg_3MnNi_2 phase possesses a strong hybridization between Mn and Mg, Ni atomic orbits under simultaneously retaining the strong bonding among Mg s, Mg p and Ni d electrons. Based on the calculated results, the stability of phases gradually decreases along the sequence pure Mg_2Ni phase > Mg_3MnNi_2 phase > Mn-substitution doped Mg_2Ni phase.

1. Introduction

Mg_2Ni is considered to be one of the most promising hydrogen storage alloys, because of its lightweight, low cost and high theoretical gravimetric hydrogen storage capacity (3.6 mass%, assuming the formation of Mg_2NiH_4). Besides, it can absorb and desorb hydrogen at moderate temperatures and pressures. However, the poor hydriding/dehydriding kinetics and high thermodynamical stability of Mg_2NiH_4 (requiring 280 °C for 1 bar hydrogen [1]) become the obstacle for the practical use for hydrogen storage. Mn, as a ternary element, has been experimentally added into Mg_2Ni for improving its hydrogen storage properties. Different literatures reported different substitution methods. Some authors used Mn to substitute Ni [2–3], while others used Mn to substitute Mg in Mg_2Ni [4–5]. However, these literatures only focus on the nominal change of initial elemental composition after Mn-substitution, which does not mean that the real substitution of lattice sites of atoms (Mg or Ni) in Mg_2Ni alloy is generated. In theoretical aspect, Jurczyk et al. [6] carried out the total energy calculations for $Mg_{11/6}Mn_{1/6}Ni$ and indicated that the impurity atoms Mn preferred Mg(6i) position. However, the total energy calculations of the substitution of Ni by Mn were not reported and not compared with that of Mg, too. Therefore, whether Mn prefers to substitute Ni or Mg lattice sites in Mg_2Ni as well as the specific position of substitution is not clear. Many works have been dedicated to the investigation of electronic and structural properties of high temperature (HT)-Mg_2NiH_4 (cubic) [7–8] and low temperature (LT)-Mg_2NiH_4 (monoclinic) [8–10]. Takahashi et al. [11] studied the electronic structure of Mg_2Ni intermetallic hydride containing a variety of alloying elements (V, Cr, Fe, Co, Cu, Zn) by the DV-Xα cluster method. van Setten et al. [12] investigated the effects of transition metal (Fe, Co, Cu) doping of Mg_2NiH_4 by first principles density functional theory calculations. However, there are very few reports on the theoretical calculation on the substitutional doping of Mn in Mg_2Ni phase and this subject needs to be further studied.

We have reported the synthesis of the new nanocrystalline Mg_3MnNi_2 phase by the one-step mechanical alloying in argon atmosphere [13]. This phase, as a new hydrogen storage alloy, has been proved to possess better electrochemical hydrogen storage properties. To the best of our knowledge, the electronic structure investigation on Mg_3MnNi_2 phase has not been reported.

In this work, we study the substitutional doping of Mn in Mg_2Ni phase as well as the electronic structure of Mg_3MnNi_2 phase by first principles density functional theory calculations. The preferable site of substitution of Mn in Mg_2Ni lattice has been determined by total energy calculation, which provides a guide for using the method of elemental substitution to improve the hydrogen storage

---

* Corresponding authors. Tel.: +33 3 84583545; fax: +33 3 84583000.
E-mail addresses: liwu.huang@utbm.fr (L.W. Huang), omar.elkedim@utbm.fr (O. Elkedim).

0925-8388/$ – see front matter © 2010 Elsevier B.V. All rights reserved.
doi:10.1016/j.jallcom.2010.08.129

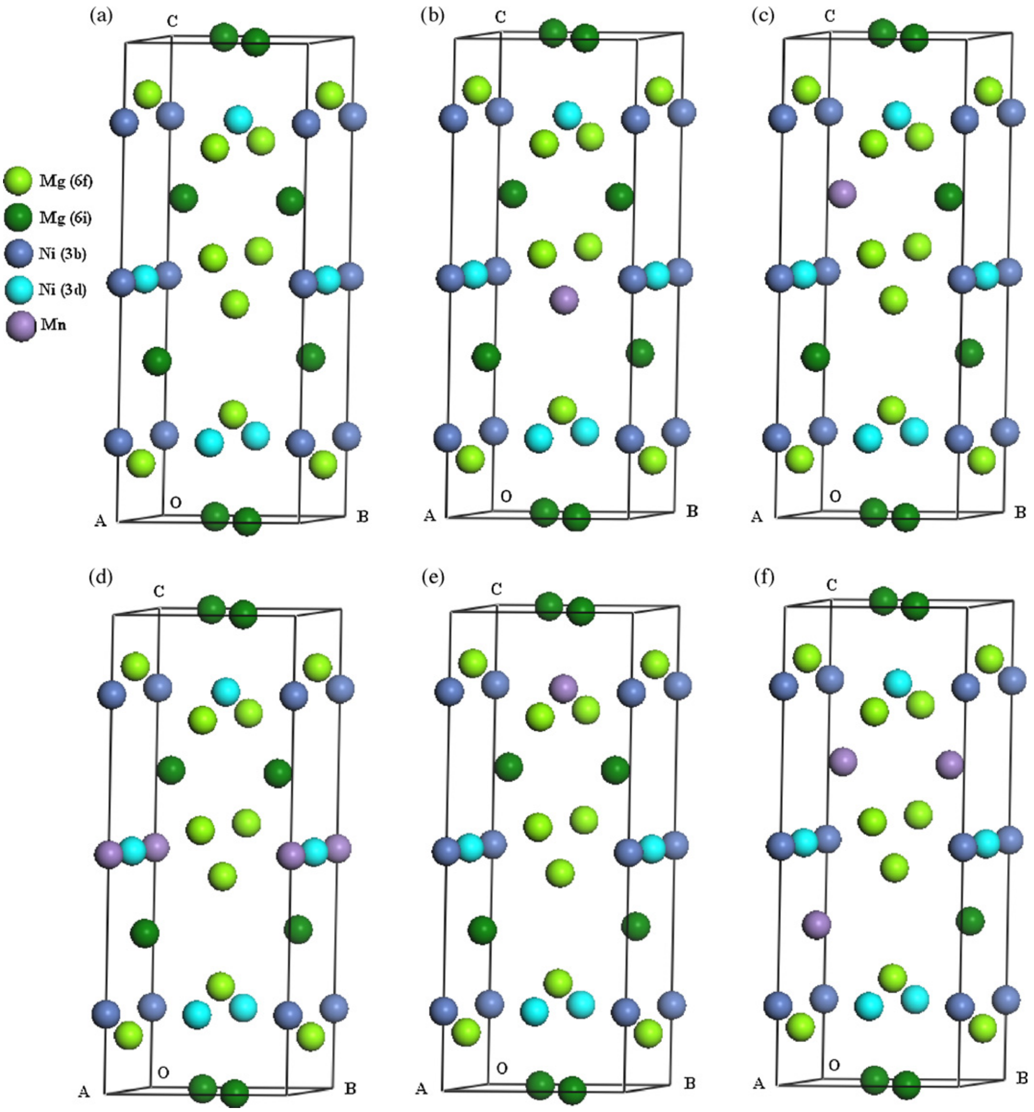

Fig. 1. Models of the unit cell of Mg_2Ni (a), $Mg_{11}Mn_{Mg(6f)}Ni_6$ (b), $Mg_{11}Mn_{Mg(6i)}Ni_6$ (c), $Mg_{12}Mn_{Ni(3b)}Ni_5$ (d), $Mg_{12}Mn_{Ni(3d)}Ni_5$ (e) and $Mg_9Mn_{3Mg(6i)}Ni_6$ (f).

properties of Mg_2Ni intermetallic compound. Furthermore, the change of structural stability from the Mn-substitution doped Mg_2Ni phase to Mg_3MnNi_2 phase is studied for explaining the formation process of Mg_3MnNi_2 phase.

2. Computational models and method

The structure of Mg_2Ni phase is shown in Fig. 1a. Its unit cell belongs to the space group $P6_222$ with lattice parameters $a = 5.216(6)$ Å, $c = 13.20(6)$ Å [14]. The Mg_2Ni unit cell contains 6 formula units, which can be expressed as $Mg_{12}Ni_6$. The 12 Mg atoms occupy 6f and 6i lattice sites, while 6 Ni atoms occupy 3b and 3d lattice sites. The different lattice sites are denoted by the balls in different colors as shown in Fig. 1a. To investigate the effects of substitutional doping, a Mn atom is introduced into the Mg_2Ni unit cell to substitute the atom at Mg(6f), Mg(6i), Ni(3b) and Ni(3d) lattice sites, respectively. The corresponding doped unit cells are presented in Fig. 1b–e (In Fig. 1d, only one fourth of each Mn atom located at the edges of lattice belongs to the doped unit cell).

The unit cell of Mg_3MnNi_2 phase is shown in Fig. 2a. It has a cubic symmetry (space group *Fd*-3*m*) with lattice parameter $a = 11.564$ Å [15]. Each unit cell contains 16 formula units of Mg_3MnNi_2, namely $Mg_{48}Mn_{16}Ni_{32}$. 48 Mg atoms, 16 Mn atoms and 32 Ni atoms occupy Mg(48f), Mn(16d) and Ni(32e) lattice sites, respectively. In order to increase the computational efficiency, the primitive cell shown in Fig. 2b is used in the calculation. It has 12 Mg atoms, 4 Mn atoms and 8 Ni atoms, namely $Mg_{12}Mn_4Ni_8$. By replacing 3 Mg atoms with 3 Mn atoms in the Mg_2Ni unit cell (shown in Fig. 1f), the corresponding chemistry formula $Mg_9Mn_3Ni_6$ is obtained, namely 3 formula units of Mg_3MnNi_2, which shows the same composition as that of the new Mg_3MnNi_2 phase. Because of the difference between Mg_2Ni lattice (space group $P6_222$ [14]) and Mg_3MnNi_2 lattice (space group *Fd*-3*m* [15]), the size of $Mg_9Mn_3Ni_6$ phase (based on Mg_2Ni unit cell) is different from that of the primitive cell of Mg_3MnNi_2 phase. However, their same chemical composition makes it possible to compare the stability of different structures (This has a similarity with the allotropy).

The calculation in this work has been carried out using the CASTEP programme [16], which is a first principles quantum mechanical code based on the density functional theory. It employs plane-wave basis sets to treat valence electrons and pseudopotentials to approximate the potential field of ionic cores (including nuclei and tightly bond core electrons) [17]. The Perdew–Burke–Ernzerhof (PBE) [18] generalized gradient approx-

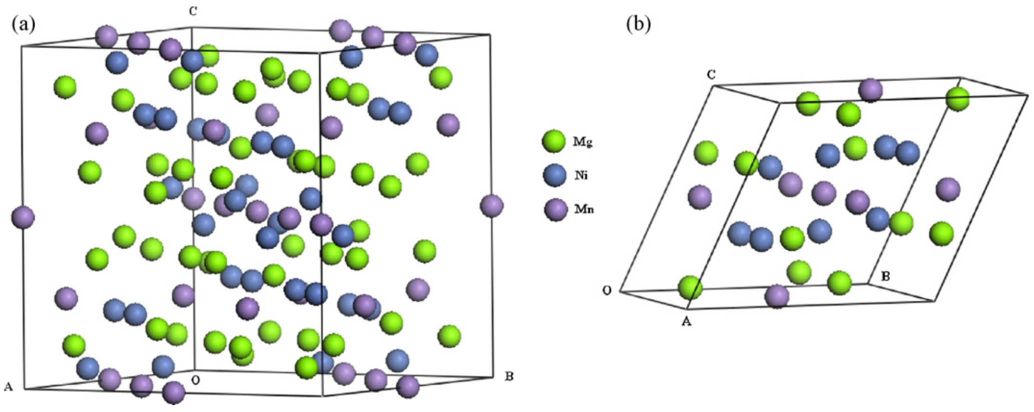

Fig. 2. Models of the unit cell (a) and primitive cell (b) of Mg_3MnNi_2 phase.

Table 1
Experimental and calculated structural parameters of Mg_2Ni and Mg_3MnNi_2 phase.

Compound	Lattice constants (Å)			Atom site	Fractional coordinates					
		Experimental	Calculated		Experimental			Calculated		
Mg_2Ni ($P6_222$)	*a*	5.216(6) [14]	5.218	Mg(6f)	0.5	0	0.1149(2) [14]	0.5	0	0.1163
	c	13.20(6)	13.246	Mg(6i)	0.1635(6)	0.327	0	0.1642	0.3284	0
				Ni(3b)	0	0	0.5	0	0	0.5
				Ni(3d)	0.5	0	0.5	0.5	0	0.5
Mg_3MnNi_2 (Fd-$3m$)	*a*	11.564 [15]	11.549	Mg(48f)	0.3239	0.125	0.125 [15]	0.3245	0.125	0.125
				Mn(16d)	0.5	0.5	0.5	0.5	0.5	0.5
				Ni(32e)	0.70529	0.70529	0.70529	0.70534	0.70534	0.70534

The digits in parentheses for experimental lattice constants and fractional coordinates are standard deviations.

imation (GGA) exchange and correlation potential was used in the calculations. The transition metals (Ni, Mn) were treated by spin polarized calculation. Ultrasoft pseudopotentials [17] in reciprocal space were used to replace the core electrons. We have tested the dependence of the total energy on the energy cutoff values and the *k*-point sets. For example, for Mg_2Ni unit cell, when the energy cutoff is higher than 380 eV and the *k*-point sets are beyond $6 \times 6 \times 2$, the change in total energy is less than 1.64 meV/atom. In consideration of computational cost, all the geometry optimization calculations were performed with a 380 eV energy cutoff. The corresponding *k*-point sets are $6 \times 6 \times 2$ for pure and Mn-doped Mg_2Ni unit cell and $4 \times 4 \times 4$ for Mg_3MnNi_2 primitive cell, respectively. The convergence criteria were set at 5.0×10^{-6} eV/atom for energy change, 0.01 eV/Å for maximum force, 0.02 GPa for maximum stress and 5.0×10^{-4} Å for maximum displacement.

The enthalpy of formation of a compound can be defined as the difference between its total energy and the energies of its constituent elements in their stable states (referred to the elementary substances). The zero-point energy (ZPE) contributions are significant in reactions where hydrogen molecules are adsorbed or desorbed [12]. The reactions investigated in this work do not include hydrogen. Thus, the ZPE contributions are not considered in this study. Therefore, for a lattice containing *x* Mg atoms, *y* Mn atoms and *z* Ni atoms, the enthalpy of formation is given by:

$$\Delta_f H = E_{\mathrm{tot}}(\mathrm{Mg}_x\mathrm{Mn}_y\mathrm{Ni}_z) - [xE(\mathrm{Mg}) + yE(\mathrm{Mn}) + zE(\mathrm{Ni})] \tag{1}$$

where $\Delta_f H$ and E_{tot} refer to the enthalpy of formation and total energy of the compound, respectively. E(Mg), E(Mn) and E(Ni) are the single atomic energies of the hcp-Mg, α-Mn and fcc-Ni in the solid state, respectively. The enthalpy of formation can be used to demonstrate whether and how much a compound structure is favored over its constituent elements in thermodynamics.

3. Results and discussion

3.1. Enthalpy of formation

At first, calculations of both Mg_2Ni and Mg_3MnNi_2 crystals were performed with full optimization of both the lattice parameters and the coordinates of all atoms based on the experimentally confirmed structure. The calculated values are listed in Table 1 and compared with the experimental data. This table shows that the difference between calculated and experimental values is below 1.3% for all results, which indicates that present calculations are in good agreement with the experimental results. As shown in Table 2, the

Table 2
Total energy and enthalpy of formation of calculated models.

	Total energy (eV)		Enthalpy of formation (eV)		
	Unit cell	Primitive cell	Unit cell	Per Mg_3MnNi_2 formula unit	Per atom
Mg_2Ni	−19817.2794		−3.2691		−0.1816
$Mg_{11}Mn_{Mg(6f)}Ni_6$	−19496.4273		−2.7273		−0.1515
$Mg_{11}Mn_{Mg(6i)}Ni_6$	−19496.4777		−2.7777		−0.1543
$Mg_{12}Mn_{Ni(3b)}Ni_5$	−19115.3243		−2.1059		−0.1170
$Mg_{12}Mn_{Ni(3d)}Ni_5$	−19115.3679		−2.1495		−0.1194
Mg_3MnNi_2		−25141.5880		−1.0372	−0.1729
$Mg_9Mn_{3Mg(6i)}Ni_6$	−18854.7660			−0.5622	−0.0937

calculated enthalpy of formation of Mg_2Ni unit cell is −3.2691 eV, which can be transferred into −52.57 kJ/mol Mg_2Ni formula unit. This value is close to −51.9 kJ/mol reported in Ref. [19].

In order to study the effects of substitutional doping of Mn in Mg_2Ni phase, a Mn atom is added into Mg_2Ni unit cell to substitute a Mg (or Ni) atom at the positions 6f and 6i (or 3b and 3d), respectively. As shown in Table 2, the chemical formulae of the Mn-doped Mg_2Ni unit cells are expressed as $Mg_{11}Mn_{Mg(6f)}Ni_6$, $Mg_{11}Mn_{Mg(6i)}Ni_6$, $Mg_{12}Mn_{Ni(3b)}Ni_5$ and $Mg_{12}Mn_{Ni(3d)}Ni_5$, respectively. The enthalpy of formation is fundamental for evaluating the structural stability. The calculated enthalpies of formation per unit cell of the pure and Mn-doped Mg_2Ni unit cell are also tabulated in Table 2. It can be obtained that Mg_2Ni has the most negative enthalpy of formation, indicating that it is the most stable structure in thermodynamics. However, the Mn-substitutions for Mg or Ni atom in Mg_2Ni phase decrease the stability of Mg_2Ni phase because of the less negative enthalpies of formation in comparison with pure Mg_2Ni phase. We have reported that during the mechanical alloying of elemental powders of Mg, Ni and Mn, the first appearing phase was Mg_2Ni and it was difficult for Mn to substitute Ni site in Mg_2Ni lattice structure [13]. The present calculated enthalpy of formation shows that pure Mg_2Ni phase is more favored in thermodynamics than the Mn-doped phases, which is in good agreement with the phenomenon found in Ref. [13]. In addition, the enthalpies of formation of $Mg_{11}Mn_{Mg(6f)}Ni_6$ and $Mg_{11}Mn_{Mg(6i)}Ni_6$ are −2.7273 eV and −2.7777 eV, respectively, both of which are more negative than those of $Mg_{12}Mn_{Ni(3b)}Ni_5$ (−2.1059 eV) and $Mg_{12}Mn_{Ni(3d)}Ni_5$ (−2.1495 eV). Therefore, the Mn atom prefers to substitute Mg in Mg_2Ni lattice in comparison with Ni. Furthermore, between Mg(6f) and Mg(6i) lattice sites, it is more favorable for Mn atom to replace the Mg(6i) position due to the most negative enthalpy of formation of −2.7777 eV for $Mg_{11}Mn_{Mg(6i)}Ni_6$ among the four Mn-doped phases. As a result, the calculated enthalpy of formation confirms that the most preferable site of substitution of Mn in Mg_2Ni lattice is Mg(6i) position. This can provide a guide for using the method of elemental substitution to improve the hydrogen storage properties of Mg_2Ni intermetallic compound. Takahashi et al. [11] reported that both the Ni–H and the Ni–Mg atomic interactions were found to affect directly the phase stability of the hydride. As mentioned above, the Mn-substitutions for Mg or Ni atom in Mg_2Ni phase decrease the stability of Mg_2Ni phase, which indicates that the Ni–Mg atomic interactions are weakened (Electronic structure calculation to be introduced in Section 3.2 will also further confirm this.). Therefore, Mn-substitutions for Mg or Ni atom in Mg_2Ni phase are probably favorable for decreasing the stability of the hydride. Yang et al. [3] found that replacement of Ni in Mg_2Ni by Mn lowered the decomposition plateau pressure. Jurczyk et al. [6] obtained an enhanced discharge capacity by substituting Mg with Mn in Mg_2Ni alloy. Kohno and Kanda [4] reported that as a result of substitution of Mg with Mn, absorption of hydrogen occurred at lower temperature, which indicates that substituting Mg with Mn can overcome the poor hydriding/dehydriding performance of Mg_2Ni alloy. As a result, the hydrogen storage properties can be tailored by appropriate designing of Mn-substitution.

In order to study the change of structural stability from the Mn-substitution doped Mg_2Ni phase to Mg_3MnNi_2 phase for explaining the formation process of Mg_3MnNi_2 phase, 3 Mn atoms substitute 3 Mg atoms at Mg(6i) position in the Mg_2Ni unit cell. And then the corresponding chemistry formula $Mg_9Mn_{3Mg(6i)}Ni_6$ is obtained, namely 3 formula units of Mg_3MnNi_2, which shows the same composition as that of the new Mg_3MnNi_2 phase (As mentioned above, the most preferable site of substitution of Mn is Mg(6i). Thus the $Mg_9Mn_{3Mg(6i)}Ni_6$ structure is preferred. For other possible configurations, such as $Mg_9Mn_{2Mg(6i)}Mn_{Mg(6f)}Ni_6$, $Mg_9Mn_{Mg(6i)}Mn_{2Mg(6f)}Ni_6$ and $Mg_9Mn_{3Mg(6f)}Ni_6$ their structures have also been calculated and show less negative enthalpies of formation than $Mg_9Mn_{3Mg(6i)}Ni_6$, which further confirms that the $Mg_9Mn_{3Mg(6i)}Ni_6$ is more stable. The increase of substitution amount of Mn atom for Mg atom at Mg(6f) position weakens the structural stability. Therefore, the $Mg_9Mn_{3Mg(6i)}Ni_6$ structure is selected to compare with the new Mg_3MnNi_2 phase). The enthalpies of formation per Mg_3MnNi_2 formula unit for $Mg_9Mn_{3Mg(6i)}Ni_6$ phase and Mg_3MnNi_2 phase are listed in Table 2. It can be seen that the enthalpy of formation of Mg_3MnNi_2 phase (−1.0372 eV) is far below than that of $Mg_9Mn_{3Mg(6i)}Ni_6$ phase (−0.5622 eV), which indicates that the Mg_3MnNi_2 phase is more stable than $Mg_9Mn_{3Mg(6i)}Ni_6$ phase. This is the reason why Mg_3MnNi_2 phase appeared after long time of milling rather than $Mg_9Mn_{3Mg(6i)}Ni_6$ phase [13]. The enthalpies of formation per atom for all structures in Table 2 show that the stability of phase gradually decreases along the sequence pure Mg_2Ni phase > Mg_3MnNi_2 phase > Mn-substitution doped Mg_2Ni phase, which is consistent with the experimental results (During the mechanical alloying of elemental powders of Mg, Ni and Mn, at first, the Mg_2Ni phase appeared, and then Mg_3MnNi_2 phase. No Mn-substitution doped Mg_2Ni phase was observed) in Ref. [13].

3.2. *Electronic structure*

Analysis of total and partial density of states (DOS and PDOS) of the pure and doped phase has been performed to study the electronic structure mechanism on the change of structural stability. Fig. 3a exhibits the DOS and PDOS of pure Mg_2Ni phase. It can be seen that the main bonding peaks are located at the energy range between −7.8 eV and Fermi level E_F. The highest peak at −1.4 eV is mainly contributed by the Ni *d*, the main part, Mg s, Mg p and a few Ni p electrons. The bonding peaks between −6 eV and −4 eV originate from the contribution of the electrons of Mg s, Mg p and Ni s, Ni p orbits. The bonding peaks from −7.8 eV to −6 eV are dominated by Mg s and a few Ni s electrons. This indicates that there is a wide hybridization between Mg and Ni atomic orbits, among which, the strong bonding between Mg s, Mg p and Ni d electrons is dominant and controls the structural stability of Mg_2Ni phase. The DOS of $Mg_{11}Mn_{Mg(6f)}Ni_6$ and $Mg_{11}Mn_{Mg(6i)}Ni_6$ are nearly the same (The DOS of $Mg_{12}Mn_{Ni(3b)}Ni_5$ and $Mg_{12}Mn_{Ni(3d)}Ni_5$ are also nearly the same.), which is consistent with the little difference of the enthalpies of formation between them as calculated above. Therefore, only the DOS for the preferable Mg(6i) and Ni(3d) position for the substitution of Mn for Mg and Ni, respectively, are chosen to be shown in Fig. 3b and c for comparison. For Mn-doped Mg_2Ni unit cells, the differences of DOS shown in Fig. 3b and c can be seen: (1) compared with the pure Mg_2Ni unit cell, the altitude of the bonding peaks of Mg s, Mg p and Ni d decreases between −4.0 eV and E_F for $Mg_{11}Mn_{Mg(6i)}Ni_6$ and $Mg_{12}Mn_{Ni(3d)}Ni_5$; (2) Due to the Mn-substitution, the Mn s, Mn p and Mn d orbits participate in bonding with Ni and Mg atomic orbits in the energy region −4.0 to 0 eV. The first difference indicates that the interaction among Mg s, Mg p and Ni d orbits is weakened, which will destabilize the unit cells. The Mg-Ni atomic interaction is the most dominant, because it supports the structural framework of unit cell. Therefore, though there is a bonding among Mg, Ni and Mn atoms, the decrease of Mg-Ni atomic interaction lowers the stability of Mn-doped phases, which is consistent with the calculated results of enthalpy of formation. Fig. 3f shows the spin-resolved DOS for Mn d states. Red and green curves denote up spin and down spin, respectively. It can be seen that because of spin polarization, the Mn d states are mainly located below and above E_F for the up spin and down spin, respectively. However, the highest bonding peak of Mn d up spin state for $Mg_{11}Mn_{Mg(6i)}Ni_6$ is pushed to a lower energy (−2.95 eV) than that (−2.65 eV) of $Mg_{12}Mn_{Ni(3d)}Ni_5$. The hybridization among Mg, Ni and Mn at lower energy region is favorable for the struc-

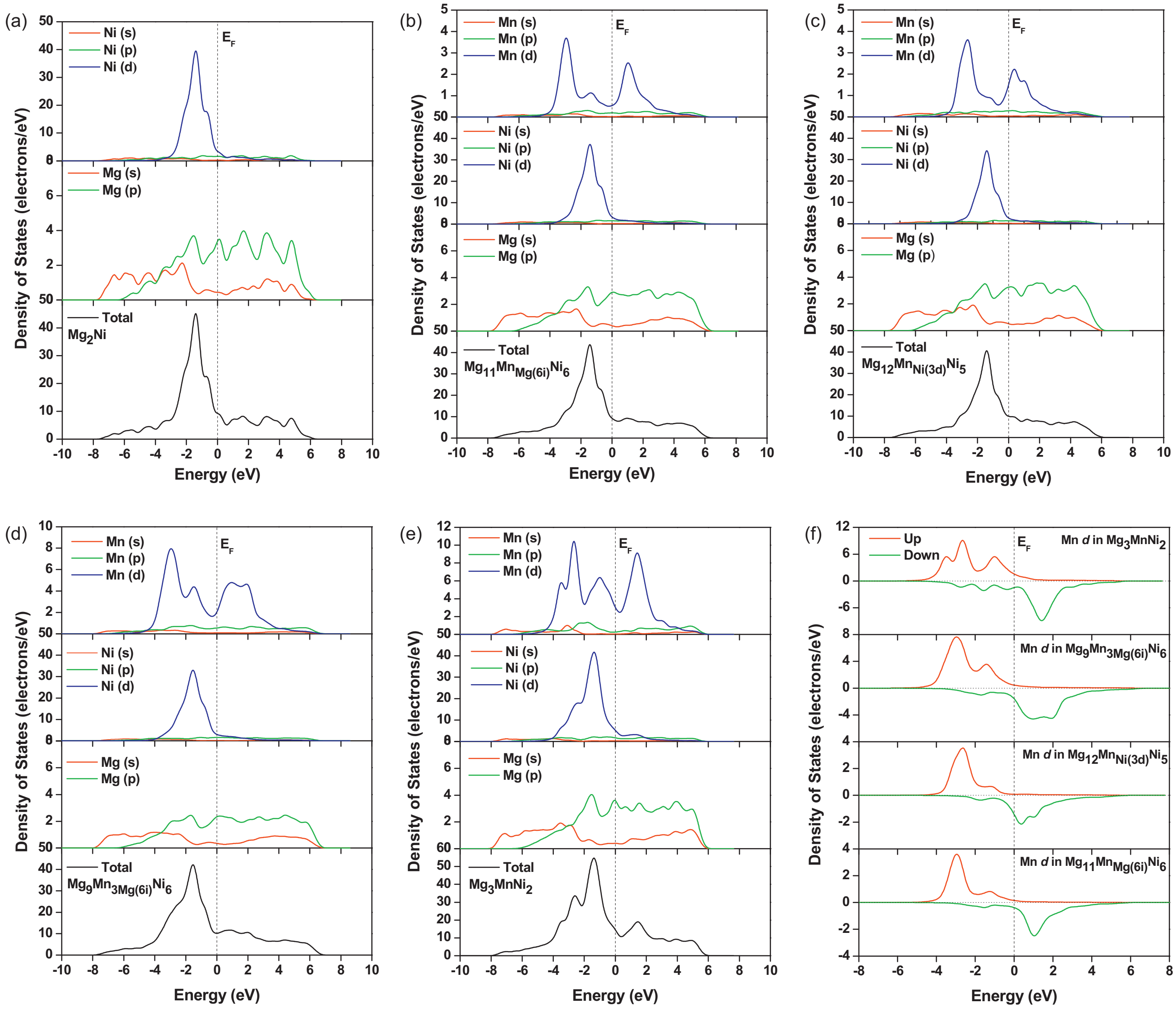

Fig. 3. Total and partial density of states of Mg_2Ni (a), $Mg_{11}Mn_{Mg(6i)}Ni_6$ (b), $Mg_{12}Mn_{Ni(3d)}Ni_5$ (c), $Mg_9Mn_{3Mg(6i)}Ni_6$ (d), Mg_3MnNi_2 (e) and spin-resolved DOS for Mn d states (f). The vertical dashed line represents the Fermi level E_F.

tural stability. As a result, $Mg_{11}Mn_{Mg(6i)}Ni_6$ unit cell is more stable than $Mg_{12}Mn_{Ni(3d)}Ni_5$ unit cell, which is in agreement with the calculated results of enthalpy of formation. After increasing the amount of substitution of Mn, the DOS of $Mg_9Mn_{3Mg(6i)}Ni_6$ unit cell is obtained as shown in Fig. 3d. Compared with Fig. 3a–c, its altitude of the bonding peaks of Mg s, Mg p and Ni d significantly decreases between −4.0 eV and E_F. Furthermore, as shown in Fig. 3f, there are lots of Mn d down spin states above E_F. Therefore, $Mg_9Mn_{3Mg(6i)}Ni_6$ unit cell is the least stable among the Mn-doped phases. In contrast, the cubic Mg_3MnNi_2 phase that has the same composition with $Mg_9Mn_{3Mg(6i)}Ni_6$ unit cell is rather stable. As shown in Fig. 3e: (1) its altitude of the bonding peaks of Mg s, Mg p and Ni d is nearly the same with that of pure Mg_2Ni phase; (2) majority of Mn d states are below E_F, which is beneficial for making a strong bonding with Mg and Ni atoms; (3) the main and high bonding peaks of Mg p, Ni d and Mn d electrons are superimposed with each other very well below E_F, which implies a strong interaction. Therefore, Mg_3MnNi_2 phase possesses high stability, which is in agreement with the result obtained in the calculation of enthalpy of formation.

4. Conclusions

The substitutional doping of Mn in Mg_2Ni phase and the electronic structure of Mg_3MnNi_2 phase have been investigated by first principles density functional theory calculations. Based on this study, the following conclusions can be obtained: (1) The calculated lattice parameters and atomic coordinates are in good agreement with the experimental results. The calculation of enthalpy of formation shows that pure Mg_2Ni phase is more favored in thermodynamics than the Mn-dope phases. The possibility of the site of Mn-substitution in Mg_2Ni lattice has been confirmed to be Mg(6i) > Mg(6f) > Ni(3d) > Ni(3b) positions. The constructed $Mg_9Mn_{3Mg(6i)}Ni_6$ unit cell is proved to be less stable. In contrast, the cubic Mg_3MnNi_2 phase that has the same composition as that of $Mg_9Mn_{3Mg(6i)}Ni_6$ structure possesses good stability. The stability of phases gradually decreases along the sequence pure Mg_2Ni phase > Mg_3MnNi_2 phase > Mn-substitution doped Mg_2Ni phase, which is consistent with the experimental results; (2) Analysis of density of states (DOS) indicates that the strong hybridization between Mg s, Mg p and Ni d electrons is dominant in controlling the structural stability of pure and Mn-doped Mg_2Ni phases. The

Mn-substitution for Mg and Ni atoms in Mg_2Ni unit cell weakens the interaction between Mg s, Mg p and Ni d electrons. The Mn d states in Mn-doped phases and Mg_3MnNi_2 phase are mainly located below and above E_F for the up spin and down spin, respectively. The bonding among Ni d and Mg s, Mg p electrons in $Mg_9Mn_{3Mg(6i)}Ni_6$ phase is significantly decreased. The cubic Mg_3MnNi_2 phase possesses a strong hybridization between Mn and Mg, Ni atomic orbits under simultaneously retaining the strong bonding between Mg s, Mg p and Ni d electrons. The results of analysis of DOS are in agreement with that of calculation of enthalpies of formation.

Acknowledgments

This work is supported by China Scholarship Council (China) and UTBM (France) in the framework of UT-INSA project (2008). The authors would like to thank S. Guessasma from INRA Nantes (France) for providing the CASTEP programme and computational assistance.

References

[1] L. Schlapbach, A. Züttel, Nature 414 (2001) 353–358.
[2] J. Woo, K. Lee, J. Electrochem. Soc. 146 (1999) 819–823.
[3] H.B. Yang, H.T. Yuan, J.T. Ji, H. Sun, Z.X. Zhou, Y.S. Zhang, J. Alloys Compd. 330–332 (2002) 640–644.
[4] T. Kohno, M. Kanda, J. Electrochem. Soc. 144 (1997) 2384–2388.
[5] A. Gasiorowski, W. Iwasieczko, D. Skoryna, H. Drulis, M. Jurczyk, J. Alloys Compd. 364 (2004) 283–288.
[6] M. Jurczyk, L. Smardz, A. Szajek, Mater. Sci. Eng. B 108 (2004) 67–75.
[7] G.N. García, J.P. Abriata, J.O. Sofo, Phys. Rev. B 59 (1999) 11746–11754.
[8] J. Zhang, D.W. Zhou, L.P. He, P. Peng, J.S. Liu, J. Phys. Chem. Solids 70 (2009) 32–39.
[9] W.R. Myers, L.W. Wang, T.J. Richardson, M.D. Rubin, J. Appl. Phys. 91 (2002) 4879–4885.
[10] P.V. Jasen, E.A. Gonzalez, G. Brizuela, O.A. Nagel, G.A. González, A. Juan, Int. J. Hydrogen Energy 32 (2007) 4943–4948.
[11] Y. Takahashi, H. Yukawa, M. Morinaga, J. Alloys Compd. 242 (1996) 98–107.
[12] M.J. van Setten, G.A. de Wijs, G. Brocks, Phys. Rev. B 76 (2007) 075125.
[13] L.W. Huang, O. Elkedim, M. Jarzebski, R. Hamzaoui, M. Jurczyk, Int. J. Hydrogen Energy 35 (2010) 6794–6803.
[14] J. Schefer, P. Fischer, W. Hälg, F. Stucki, L. Schlapbach, J.J. Didisheim, K. Yvon, A.F. Andresen, J. Less-Common Met 74 (1980) 65–73.
[15] PDF No. 00-057-0388, International Centre for Data Diffraction.
[16] S.J. Clark, M.D. Segall, C.J. Pickard, P.J. Hasnip, M.J. Probert, K. Refson, M.C. Payne, Z. Kristallogr. 220 (2005) 567–570.
[17] D. Vanderbilt, Phys. Rev. B 41 (1990) 7892–7895.
[18] J.P. Perdew, K. Burke, M. Ernzerhof, Phys. Rev. Lett. 77 (1996) 3865–3868.
[19] O. Kubaschewski, C.B. Alcock, Metallurgical Thermochemistry, in: International Series on Materials Science and Technology, vol.24, 5th Ed., Pergamon Press, Oxford, 1979.